

# The density of small tight junction pores varies among cell types and is increased by expression of claudin-2

Christina M. Van Itallie<sup>1,\*</sup>, Jennifer Holmes<sup>2</sup>, Arlene Bridges<sup>3</sup>, Jody L. Gookin<sup>4</sup>, Maria R. Coccaro<sup>4</sup>, William Proctor<sup>3</sup>, Oscar R. Colegio<sup>5</sup> and James M. Anderson<sup>2</sup>

<sup>1</sup>Department of Medicine, <sup>2</sup>Cell and Molecular Physiology and <sup>3</sup>School of Pharmacy, University of North Carolina, Chapel Hill, NC 27599, USA

<sup>4</sup>Department of Molecular Biomedical Sciences, North Carolina State University, Raleigh, NC 27695, USA

<sup>5</sup>Department of Dermatology, Yale University School of Medicine, New Haven, CT 06510, USA

\*Author for correspondence (e-mail: vitallie@med.unc.edu)

Accepted 4 November 2007

Journal of Cell Science 121, 298–305 Published by The Company of Biologists 2008

doi:10.1242/jcs.021485

## Summary

Epithelial tight junctions contain size- and charge-selective pores that control the paracellular movement of charged and noncharged solutes. Claudins influence the charge selectivity and electrical resistance of junctions, but there is no direct evidence describing pore composition or whether pore size or density differs among cell types. To characterize paracellular pores independent of influences from charge selectivity, we profiled the ‘apparent permeabilities’ ( $P_{app}$ ) of a continuous series of noncharged polyethylene glycols (PEGs) across monolayers of five different epithelial cell lines and porcine ileum. We also characterized  $P_{app}$  of high and low electrical resistance MDCK cell monolayers expressing heterologous claudins.  $P_{app}$  profiling confirms that the paracellular barrier to noncharged solutes can be modeled as two distinct pathways: high-capacity small pores and a size-independent pathway allowing flux of larger solutes. All cell lines and ileum share a pore aperture of radius 4 Å. Using  $P_{app}$  of a PEG of radius 3.5 Å to report the relative pore number provides the novel insight that pore density along the junction varies among

cell types and is not necessarily related to electrical resistance. Expression of claudin-2 results in a selective increase in pore number but not size and has no effect on the permeability of PEGs that are larger than the pores; however, neither knockdown of claudin-2 nor overexpression of several other claudins altered either the number of small pores or their size. We speculate that permeability of all small solutes is proportional to pore number but that small electrolytes are subject to further selectivity by the profile of claudins expressed, explaining the dissociation between the  $P_{app}$  for noncharged solutes and electrical resistance. Although claudins are likely to be components of the small pores, other factors might regulate pore number.

Supplementary material available online at  
<http://jcs.biologists.org/cgi/content/full/121/3/298/DC1>

Key words: Claudin, Tight junctions, Paracellular permeability

## Introduction

Tight junctions create paracellular barriers that, depending on local transport requirements, differ in electrical conductance, ionic charge preference and the level of permeability for uncharged solutes; these properties are collectively referred to as permselectivity. For example, electrical resistance progressively increases along both the intestine (Artursson et al., 1993) and renal tubule as the transport of large volumes of isosmotic fluids shifts to more selective transport based on high electro-osmotic gradients (Powell, 1981). The barrier is formed where strands of adhesive transmembrane proteins contact across the paracellular space, and it behaves as if perforated by pores possessing size and charge selectivity. Little is known about the molecular nature of the pores, despite the identification of many tight junction proteins. Using a continuous series of polyethylene glycols (PEGs) as permeability markers, we determined the relative number of pores as a function of their aperture and asked whether different cell types have different sizes and numbers of pores and whether expression of claudins changes these properties.

Paracellular permeability is most often measured by flux of variously sized noncharged hydrophilic tracers, including

radioactively labeled urea, mannitol, inulin and/or fluorescent dextrans of various sizes (Ghandehari et al., 1997; Sanders et al., 1995). It has been recognized for a number of years that there is a disproportionately larger permeability for compounds smaller than mannitol (Artursson et al., 1993; Knipp et al., 1997; Tavelin et al., 2003). This was most elegantly demonstrated by Watson and colleagues (Watson et al., 2001) by profiling paracellular flux across monolayers of Caco-2 and T84 cells with a continuous series of PEG oligomers. Their results clearly showed that, in these two cell lines, permeability is biphasic, consisting of a high-capacity, size-restrictive pathway and a low capacity, size-independent pathway. The high-capacity pathway behaves as a system of small pores with radii of ~4 Å. The physical basis of the low-capacity pathway is less clear. It could represent fixed (e.g. tricellular junctions) or transient breaks (e.g. during apoptosis) or a system of larger pores.

Other investigators have used a variety of techniques to determine the small pore size and have reported substantially different sizes in different cell lines, tissues and in different species. For example, Tavelin and colleagues (Tavelin et al., 2003) used a

variety of paracellular flux markers to demonstrate that the small pore radius in an intestine-like cell line called 2/4/A1 was 9 Å, whereas the Caco-2 pore size was found to be 3.7 Å. Fihn and colleagues (Fihn et al., 2000) reported that pore size is larger in intestinal crypt (50–60 Å) than in villus cells (<6 Å). He and colleagues (He et al., 1998) demonstrated larger paracellular pores in the small intestine of dog compared with human. However, none of these studies had the resolution of the PEG profile studies, which are able to determine the relative number of pores as a continuous function of size (Watson et al., 2001; Watson et al., 2005).

Along with solute flux, paracellular barrier function is commonly characterized by transepithelial electrical resistance (TER). As information has emerged about the protein components of the tight junction, many studies have demonstrated that the electrical tightness of cultured epithelial monolayers can be increased or decreased by changing the expression profiles of specific proteins (reviewed by Gonzalez-Mariscal et al., 2003; Schneeberger and Lynch, 2004). Interest has centered on the integral membrane proteins of tight junctions, particularly claudins, occludin and junctional adhesion molecules (JAMs) as these three proteins have been demonstrated to be components of the strands that can be visualized by freeze-fracture electron microscopy and that are the sites of the adhesive cell-to-cell barriers. Our studies (Van Itallie et al., 2001; Colegio et al., 2002) and those of several other groups (Amasheh et al., 2002; Yu et al., 2003; Hou et al., 2005) have demonstrated that claudins can change the TER through regulation of ionic charge selectivity. For example, expression of claudin-14 in MDCK II cells (Ben Yosef et al., 2003) increases TER fivefold by selectively decreasing paracellular permeability to cations ( $\text{Na}^+$ ) without changing permeability for anions ( $\text{Cl}^-$ ). Investigations of this type, coupled with mutational analysis of the claudin extracellular domains (Colegio et al., 2002; Hou et al., 2005; Alexandre et al., 2007), provide convincing evidence that claudins line the paracellular pores. The roles of occludin (Saitou et al., 1998; Yu et al., 2005) and JAMs (Mandell and Parkos, 2005) are understood less well.

Although paracellular flux of noncharged solutes and electrical resistance are both measures of permeation through the paracellular pathway, their relationship sometimes appears paradoxical. For example, it seems consistent that TER decreases at the same time that solute flux increases following exposure of T84 cell monolayers to interferon- $\gamma$  (Watson et al., 2005). By contrast, there are multiple examples where changing claudin levels alters TER without any coincident changes in flux for noncharged solutes (Van Itallie et al., 2001; Amasheh et al., 2002) or where changes in occludin levels increase TER and flux simultaneously (Balda et al., 1996). To better understand the relationship between TER and permeability and to begin to identify the proteins involved in the regulation of solute flux, we have adapted a method (Watson et al., 2001) for profiling the permeability of tight junctions as a function of solute size and applied it to several different cultured epithelial cell lines and tissues. Our initial aims were to determine first whether pore size and number varied among different cell types, second whether claudins influence these properties and third how pore number is related to TER. We demonstrated previously that the electrical charge on the extracellular domains of claudins influences the permeability of ions passing through the tight junction, consistent with the idea that claudins border, or are within a few Ångstroms of, the pores (Colegio et al., 2002). This led us to ask whether different claudins might differentially affect pore size and/or number. We chose to focus our study on claudin-2 (also

known as claudin 2) as this claudin has been identified as an electrically 'leaky' claudin (Furuse et al., 2001; Amasheh et al., 2002) and is concentrated in intestinal crypts (Holmes et al., 2006), where larger paracellular pores have been reported (Marcial et al., 1984). We also tested the effects of expressing claudin-4, which increases TER in MDCK II cells, and asked whether this increased TER was accompanied by a decrease in pore number or size. We found that, in all tested monolayers, the majority of solute flux occurs through pores with a common aperture radius of 4 Å. We made the novel observation that the density of small pores along the junction varies significantly among cell types. Furthermore, we found that expression of claudin-2 in MDCK cells could increase the number of small pores but that neither knockdown of claudin-2 nor expression of several other claudins could influence pore number. These findings suggest that, although claudins might be components of the small pores, other factors regulate pore number.

## Results

### Using PEGs to profile size selectivity of the paracellular pathway

In order to ask how individual tight junction proteins regulate paracellular size discrimination, we modified a method reported by Watson and colleagues (Watson et al., 2001) to determine paracellular flux of a continuous series of PEG oligomers. In our modification, we fluorescently modify the PEGs with 1-naphthyl isocyanate (1-NIC) (Rissler et al., 1998) after performing flux assays, then separate by HPLC and quantify by fluorescence emission. Each PEG is modified on the two terminal hydroxyl groups, and the signal is directly proportional to the number of molecules, regardless of size. Sample chromatograms in Fig. 1 show typical flux profiles across a Caco-2 cell monolayer. The donor compartment (Fig. 1A) contains comparable concentrations of a continuous series of PEG sizes (PEG<sub>2</sub>–PEG<sub>25</sub>), with elution time proportional to size. After 90 minutes, the profile on the acceptor side (Fig. 1B) shows strong size discrimination above an HPLC retention time (~7 minutes), corresponding to a radius of ~4 Å. Purified PEG<sub>28</sub> is added before derivatization as an internal recovery standard (far-right peak in Fig. 1). We have verified that derivatization is complete, flux is linear up to 3 hours and identical in both directions, and the filter without cells shows high permeability without size selectivity (data not shown). The smallest PEG reliably detected is of radius 2.8 Å (PEG<sub>3</sub>, HPLC position

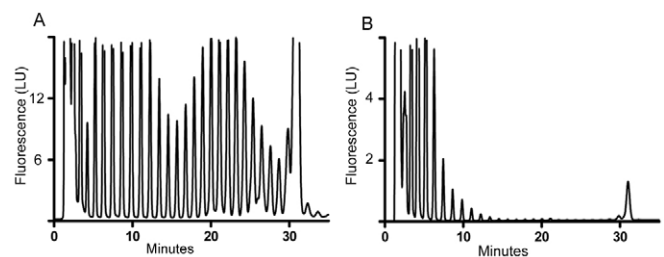


**Fig. 1.** Profile of PEG oligomers after flux across a Caco-2 monolayer reveals a sharp size discrimination. A mixture of continuous PEG oligomers (dimer to 28mer) was added to the apical compartment of monolayers cultured on semipermeable filters. Aliquots were removed from the donor (A) and acceptor (B) compartments after 90 minutes, derivatized with 1-NIC and subjected to HPLC and detected by fluorescence emission. Each peak represents a single ethylene glycol adduct size, and retention times are proportional to molecular mass. The peak visible at 31 minutes is pure PEG<sub>28</sub> added as an internal recovery standard after the flux protocol.

verified with triethylene glycol), and the largest we studied is  $\sim 7$  Å (PEG<sub>25</sub>). The hydrodynamic radii ( $r$ ) of PEG oligomers are related to molecular mass ( $M$ ) by the relationship  $r$  (Å) =  $0.29M^{0.454}$  (Ruddy and Hadzija, 1992). PEG measurements are converted to 'apparent permeability' ( $P_{app} = [dQ/dt]/[\text{area of the filter} \times \text{concentration difference}]$ ), so that they can be compared among PEG sizes and different cell types. The assay is sensitive and highly reproducible.

The number of pores but not their size differs among cell types. PEG permeability profiling offers striking insights about the size selectivity of the paracellular pathway. When  $P_{app}$  is plotted as a function of PEG radius (Fig. 2), two components or pathways are clearly revealed. The first has a steep negative slope, from which it is possible to calculate an approximate pore radius of 4 Å; this can be interpreted as a high-capacity system of small pores with a clearly defined aperture size. Solutes that are larger than the small pores are relatively more restricted and pass in a size-independent manner; the slope of  $P_{app}$  as a function of size is close to zero. This implies that their diffusion occurs through intercellular spaces that are much larger than 8 Å and that account for relatively less area than the area containing small pores. The magnitude of both pathways varies among cell types. Molecules that are smaller than the pores (PEG<sub>3</sub>-PEG<sub>5</sub>) can also pass through the nonrestrictive pathway; this contribution must be subtracted from the first phase to determine their permeability specifically through the pores as well as to derive the pore size. To correct for this contribution, the second phase ( $\geq 4$  Å) is analyzed by linear regression, and extrapolated values are subtracted from the first phase.

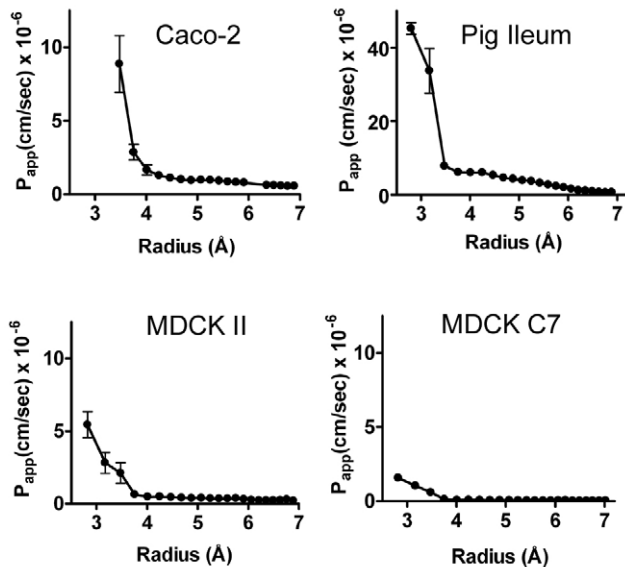


**Fig. 2.**  $P_{app}$  as a function of PEG radius in Caco-2, MDCK II and MDCK C7 monolayers and ex vivo pig ileum. All cell types show a size-restrictive pore calculated to be of radius  $\sim 4$  Å. Ileum appears to have an additional pore cut-off at  $\sim 6.5$  Å. In contrast to their similar size pore, the number of pores (reflected in the  $P_{app} < 4$  Å) is highly variable. Caco-2 cells have the largest numbers of pores as well as the greatest permeation through the size-independent pathway; MDCKII cells have an intermediate number and MDCK C7 cells have few pores and little permeation through the second pathway. T84 cells (data not shown) had a variable pore number, depending on the source of the cell line. The relative pore number in pig ileum cannot be compared with that of cell lines because of the difference in the amplified surface area in intact tissue compared with the flat cultured cell monolayers.

We have extended the published studies of the human intestinal cell lines Caco-2 and T84 (Watson et al., 2001) to include ex vivo porcine ileal mucosa and three renal tubular epithelial lines, namely porcine LLC-PK<sub>1</sub> cells (data not shown) and two clones of canine MDCK cells, low-TER MDCK II and high-TER MDCK C7 (Gekle et al., 1994; Wunsch et al., 1995) (Fig. 2). The key observations are, first, that all five cell lines have a similar pore radius of  $\sim 4$  Å. Ileum (and possibly Caco-2) has an additional cut-off of  $\sim 6.5$  Å (Fig. 2). Second, the number of pores per area of the monolayer, which is proportional to  $P_{app}$  for solutes that are of radius  $< 4$  Å, is strikingly different among cell types. It should be noted that pore number is a functional definition, not a structural one, as small pores could theoretically have open or closed probabilities that differ among the different cell lines. Third, the nondiscriminating pathway is also variable in magnitude, but less so than the small pores. We also attempted to characterize the size selectivity of HUVECs, a commonly used human umbilical vein endothelial cell line. However, despite establishing a low but detectable TER, HUVEC monolayers showed little discrimination in the range 2.3-7.0 Å, implying that their predominant paracellular spaces are larger than 7 Å.

#### Pore density along the junction differs among cell types

The difference in pore number per unit area among cell lines is not the result of differences in the linear length of junction per unit area; instead our data lead to the novel conclusion that cell types

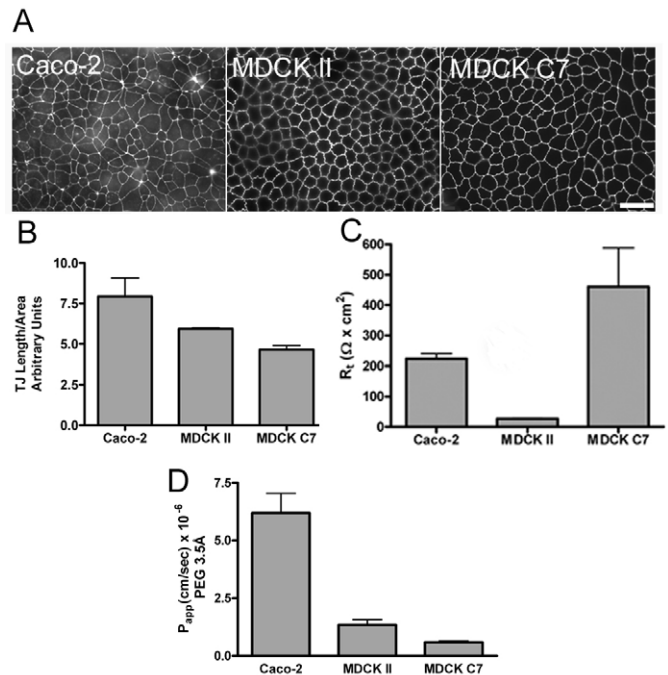


**Fig. 3.** Lack of correlation between intercellular junction length, pore number and TER. (A) Immunofluorescent localization of ZO-1 in cells grown on filters and used for TER was used to determine the length of tight junction contacts per monolayer area. Caco-2 cells are the smallest and thus have the most potential junction contact length to leak through. Bar, 12 μm. (B) Duplicate cell fields were photographed and measurements of perimeter lengths were determined using imaging software. The perimeter lengths differed by less than 30% among the three cell lines; Caco-2 monolayers contain the most and MDCK C7 the least. TER (C) was not necessarily inversely related to junction length (B) nor to pore number, as determined by  $P_{app}$  of the 3.5 Å PEG species (D).

can differ in the apparent density of pores along the junction (Fig. 3). Junction length per area was derived from monolayers immunolabeled for a marker of tight junctions and analyzed by imaging software (Fig. 3B). Caco-2 cells are slightly smaller than both clones of MDCK cells (Fig. 3A) and thus have slightly more junctional length through which PEGs can diffuse (Fig. 3B). In order to compare the relative number of pores per unit area, we compare the  $P_{app}$  for the 3.5 Å species, which should be directly proportional to the number of pores. When the  $P_{app}$  for PEG<sub>5</sub> is compared among cell types (Fig. 3D), Caco-2 monolayers are seen to have  $\geq 12$ -fold more pores per area than MDCK C7; MDCK II monolayers are intermediate. When  $P_{app}$  is corrected for differences in the length of junction per area, Caco-2 cells still contain  $\geq 7$ -fold more pores per length of junction than MDCK C7 cells; the density of pores along MDCK II cell junctions is intermediate. Microanatomical differences, including differences in tight junction strand number or tortuosity that we have not assessed might contribute to the apparent differences in pore density; however, previous electron-microscopic comparison of high-resistance (similar to C7 cells) and low-resistance MDCK cell lines did not demonstrate any anatomic difference in the morphology of the tight junctions (Stevenson et al., 1988) in spite of the observed difference in apparent TER.

TER is inversely proportional to the current that flows in response to an applied voltage; in physiologic solutions, this current is primarily carried by Na<sup>+</sup> (0.95 Å) and Cl<sup>-</sup> (1.81 Å) ions (Hille, 2001) and thus mainly conducted through the small pores. Therefore, the TER of a monolayer might be expected to be inversely related to the number of pores as defined by flux studies; however, we observed that this is not necessarily true. While MDCK C7 monolayers do have a higher TER (Fig. 3C) and fewer pores than either Caco-2 or MDCK II monolayers (Fig. 3D), Caco-2 monolayers actually have both a much higher TER and higher number of pores than MDCK II monolayers. Assuming that claudins are a major component of pores, we speculate that this apparent inconsistency results from the charge discrimination characteristics of different claudins expressed in Caco-2 versus MDCK II cells. This has an impact on TER but not the  $P_{app}$  of non-charged PEGs. TER could therefore be both a function of claudin charge selectivity and of the number of pores, each of which can vary independently.

#### Induction of claudin-2, but not claudin-4, increases the number of small pores

MDCK II and MDCK C7 monolayers differ significantly in TER and in relative pore number (Fig. 3C,D), despite having approximately the same length of junction per monolayer area. One possible reason for the difference in porosity might be a difference in the expression profiles of their tight junction proteins. Amasheh and colleagues (Amasheh et al., 2002) demonstrated that the levels of claudin-2, but not claudin-3, differ between MDCK II and C7 cells. We extended this comparison to include claudins-4 and -7, plus ZO-1, occludin and E-cadherin (Fig. 4). The largest differences were that MDCK C7 cells have much lower levels of claudin-2 (~7%) and claudin-7 (~30%) and much higher levels of claudin-4 protein (increased by more than sixfold). The immunofluorescent localizations of the various claudins in the two cell lines were similar (supplementary material Fig. S1). If one assumes that pore density is a function of the number of pore-forming claudins in a background of non-permeant strand proteins (occludin or JAM, for example), then it might be possible to alter

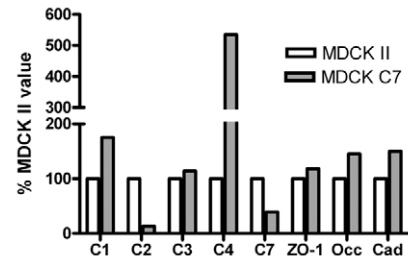


**Fig. 4.** Comparison of claudin protein expression profiles in MDCK II and MDCK C7 cells. Comparative immunoblotting was performed to determine whether the difference in TER and pore number between MDCK II and C7 cell lines could result from different claudin expression profiles. Duplicate cell monolayer filters that were used for immunofluorescent analysis (Fig. 3) were processed for immunoblots with a panel of antibodies against claudins and other junction proteins to compare relative protein levels; quantification was performed using Licor Odyssey software. Levels in MDCK C7 cells are presented relative to MDCK II levels. Most claudins, ZO-1, occludin and E-cadherin are expressed at similar levels, whereas, in C7 cells, claudin-2 is much less prevalent and claudin-4 much more prevalent.

pore number by changing the composition of the strands through expression of particular claudins. Interestingly, expression of claudin-2 in high-TER MDCK cells results in decreased TER (Furuse et al., 2001; Amasheh et al., 2002), whereas siRNA-mediated knockdown of claudin-2 in low-TER MDCK II cells increases TER (Hou et al., 2006). This led us to test the possibility that increasing levels of claudin-2 might increase the number of small pores.

PEG profiling and  $P_{app}$  were determined (Fig. 5) in MDCK II monolayers stably expressing claudins-2, -4, -14 and -18, in MDCK C7 cells expressing claudin-2 and in MDCK II cells in which expression of claudin-2 was inhibited by using RNAi. Immunoblots (Fig. 5A) reveal at least a fourfold increase in claudin-2 and claudin-4 in representative MDCK cell clones and a 90% decrease in claudin-2 in the RNAi knockdown cells; in no condition was there much change in occludin, an unrelated transmembrane protein in the strands (Fig. 5A), or in the levels of claudins-1 or -3. Induction of claudin-4 resulted in a twofold decrease in the levels of claudin-7; however, the physiological consequences of the decrease are unclear as claudin-7 is located all along the basolateral membrane of MDCK cells (supplementary material Fig. S2). The effects of expression of claudins-2 and -4 on TER have been reported previously (Colegio et al., 2003; Van Itallie et al., 2001; Amasheh et al., 2002; Hou et al., 2006); the present study confirmed that expression of claudin-2 in low-resistance MDCK II cells caused a slight increase in TER, whereas expression of the same claudin in high-resistance MDCK C7 cells resulted in a significant drop in resistance. Expression of claudin-4 and knockdown of expression of claudin-2 in MDCK II cells resulted in twofold and threefold increases in TER, respectively (Fig. 5B).

When claudin-2 is expressed in MDCK II (Fig. 5C,D) and C7 monolayers (Fig. 5D), there is a significant increase in the  $P_{app}$  for PEGs that can traverse the pore (<4 Å), whereas there is no significant change in permeability for PEGs that are larger than the pores. The finding that pore number increases in both cell lines in the face of differing effects on TER is not unexpected as additional pores would have little effect on ionic flux in the already extremely leaky Na<sup>+</sup>-selective MDCK II background but could increase both paracellular Na<sup>+</sup> flux and non-ionic permeability in the much 'tighter' C7 cell line.

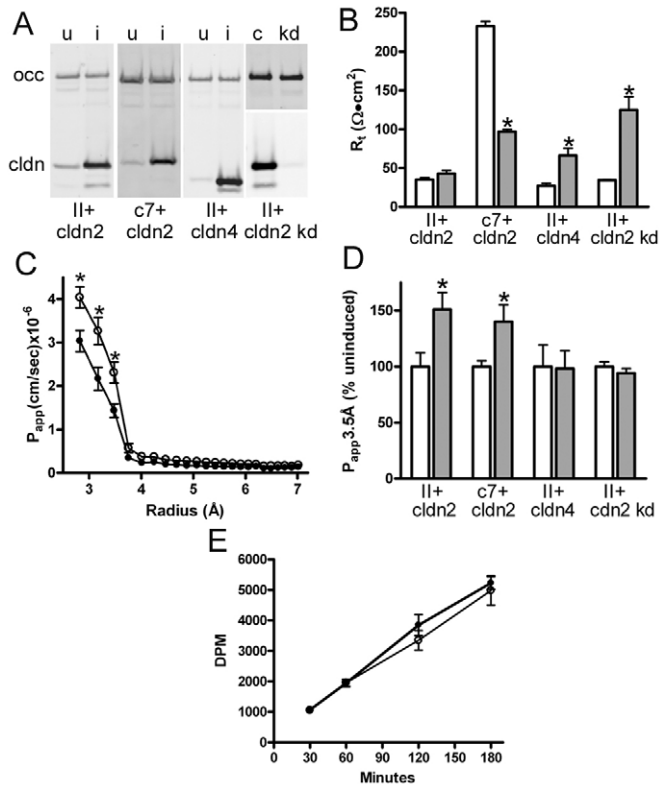


**Fig. 5.** Expression of claudin-2, but not claudin-4, in MDCK monolayers increases the number of pores. (A) Representative immunoblots from cells used for TER and  $P_{app}$  studies demonstrate at least fourfold higher levels of claudin after induction (i) compared with those in uninduced (u) cells; claudin-2 expression in knockdown (KD) cells was approximately 2-10% of control cell values; occludin (occ) levels are unchanged. Approximate molecular masses: occludin, 60 kDa; claudin-2, 22 kDa, claudin-7, 20 kDa; claudin-4, 17 kDa. (B) Induction (filled bars) of claudin-2 compared with uninduced (unfilled bars) MDCK II monolayers results in a small increase in TER, and a large drop in C7 cells. Induction (filled bars) of claudin-4 in MDCK II monolayers causes a twofold increase in TER relative to uninduced (unfilled bars) monolayers; knockdown of claudin-2 results in a threefold increase in TER (filled bars) over parental cell values (unfilled bars). (C) Induction of claudin-2 (unfilled circles) in MDCK II monolayers results in a significant increase in the  $P_{app}$  specifically for PEG sizes that are of radius  $<4 \text{ \AA}$ , compared with uninduced monolayers (filled circles). Means and s.e. of four separate clones. (D) Corrected  $P_{app}$  of the  $3.5 \text{ \AA}$  PEG<sub>5</sub> species reveals increases in pore number after inducing claudin-2 (filled bars) relative to uninduced (unfilled bars) in both MDCK II and MDCK C7 cells, but no change in MDCK II cells expressing claudin-4 or knockdown cells with decreased claudin-2 expression (means and s.e. from at least four determinations). (E) [<sup>3</sup>H]-Mannitol flux [disintegrations per minute (DPM) versus time] is unaffected by induction of claudin-2 (unfilled circles) compared with uninduced (filled circles) MDCK II monolayers.

In contrast to the effects of overexpression of claudin-2, knockdown of claudin-2 levels in MDCK II cells does not change the apparent pore number (Fig. 5D). In addition, there was no change in  $P_{app}$  profiles in MDCK II cells induced to express claudins-4 (Fig. 5D), -14 or -18 (data not shown). Morphometric analysis of the length of tight junctions before and after induction of any of the claudins did not show a significant change (data not shown). Together, these data suggest that the ability of claudin-2 to increase pore number might be a special characteristic of this claudin and that, even though knockdown of claudin-2 or overexpression of claudins-4, -14 and -18 can alter the electrical

characteristics of the pores, they do not affect pore size or number. Of note, increasing the level of claudin-2 did not alter the flux of mannitol (Fig. 5E,  $4.2 \text{ \AA}$ ), a widely used permeability marker – revealing that mannitol flux measurements detect the magnitude of the size-independent pathway but not the small pore system.

## Discussion

Our results confirm that paracellular flux can be modeled as at least two components; one consisting of high-capacity, size-restrictive pores and a second pathway that is relatively size independent, at least for substances with radii of up to  $7 \text{ \AA}$ . Our novel observations include the finding that porcine ileum and all the cell lines analyzed in this study show small pores with the same aperture size of radius  $\sim 4 \text{ \AA}$ . Furthermore, we demonstrate that the number of pores is quite variable among cell lines and does not correlate with either the length of junction or with TER. This implies that tight junctions can vary in the density of pores along the cell-cell contact. We also observed that increasing the level of claudin-2, but not -4, -14 and -18, in MDCK cells increased the number of pores without altering the pore size or significantly altering  $P_{app}$  for PEGs that are larger than the pore. Although it is possible that pore number is regulated by claudins that we have not tested, the simplest explanation for our findings is that claudins are constituents of the pores of radius  $4 \text{ \AA}$  but that, overall, pore number within a single cell type is tightly regulated, perhaps by structural constraints, by other strand proteins or by cytosolic or regulatory components.

The accuracy of our assessment of pore size is limited by our use of a single type of probe; however, the validity of the use of PEGs as flux markers has been verified by others (Watson et al., 2001). In any case, the goal of the present study was to apply a single assay to allow comparison of relative pore sizes after different experimental manipulations rather than providing a measurement of exact pore size. However, an unexpected outcome was that all cell lines that we examined, as well as pig ileum, had identical restrictive pore sizes. With the exception of the analysis of T84 and Caco-2 cells (Watson et al., 2001), there has been little systematic comparison of pore size across different experimental systems. One exception is a comparison of PEG absorption in dog, rat and human gut, which found species-specific differences in pore size (He et al., 1998). Other studies demonstrated the presence of larger pores in intestinal crypts when compared with villus cells (Fihn et al., 2000). It is possible that tissues have a more complex pore composition than the homogeneous cell lines we examined as our results in pig ileum suggest the existence of a second restrictive pore with a size cut-off of radius  $\sim 6-7 \text{ \AA}$ .

Pore size might be a function of claudin structure. As claudin expression in non-epithelial fibroblasts can recapitulate the strand morphology of tight junctions (Furuse et al., 1998), we have assumed that the tight junction barrier comprises continuous claudin polymers that organize to form paracellular pores. Many studies have now demonstrated that claudins influence paracellular ionic selectivity and TER – it would seem reasonable to assume that these would be the same pores that regulate the flux of the small PEGs. As all claudins have extracellular loops of nearly identical size, it is possible that pore size is a function of the geometry of claudin-claudin interactions and thus would be structurally similar for all claudins. We have attempted to test this hypothesis by overexpressing PMP-22, a distant member of the claudin family, which is a component not only of peripheral myelin but also of epithelial tight junctions (Notterpek et al., 2001) and which has smaller extracellular domains than are characteristic of

conventional claudins (56 compared with 77 amino acids for loop 1 plus loop 2). We found that overexpression of PMP-22 did not change the pore size in MDCK II cells; however, the overexpression was in the background of endogenous claudins and thus their presence might have defined the majority pore size. To test this more explicitly, we would need to perform these studies in a cell background where PMP-22 is the predominant claudin; this will be attempted in future experiments. It is also possible, however, in spite of the fact that claudins form the structural basis of the tight junction, and regulate paracellular ion selectivity, that the small pores measured by PEG flux represent a separate passage through the tight junction.

Even if small pore size is determined by claudin interactions, there could still be a second set (or more) of larger size-restrictive pores defined by interactions of other tight junction proteins or by modifiers of claudin-claudin interactions. The characterization of larger pores will depend on the ability to profile the paracellular permeation of species of higher molecular mass than the PEGs used in this study. Although profiling of this type will be less sensitive because of the lower capacity of this pathway, it is important as changes in the flux of larger molecules (e.g. antigens) is likely to be of great pathologic significance and is important for drug delivery.

The lack of relationship between TER and pore number was more dramatic than we had anticipated. For example, MDCK II cells, which have a fivefold lower TER than Caco-2 cells, also have fewer pores. The simplest interpretation is that TER is regulated by the ion selectivity of the pores, not just their number. In this model, tight junctions in Caco-2 cells would be expected to comprise claudins that create a high pore density and permeability for noncharged solutes but whose pores create a high TER by restricting paracellular ion permeability. Alternatively, there has long been conjecture that the paracellular pores fluctuate between an open and closed state (Claude, 1978); pores in Caco-2 cells might be regulated such that they have a higher open probability than in MDCK cells. Additionally, although claudin expression can recapitulate tight junction fibrils in fibroblasts (Furuse et al., 1998), in epithelial cells, the fibrils are known to contain at least occludin (Furuse et al., 1993) and JAM (Itoh et al., 2001). It is possible that differences in non-claudin composition or organization contribute to differences in porosity. Finally, it is also possible that PEG flux measures a separate, claudin-independent pathway through the tight junction. It is difficult to test these various ideas as we still lack basic information about how proteins in the barrier strands are organized.

Expression of claudin-2 resulted in a significant increase in small pore number with no change in pore size. This increase could be due to a change in the absolute number of small pores or might represent the ability of claudin-2 expression to modify pore characteristics such that more pores are available for noncharged solutes. It was previously speculated that the ability of claudin-2 to decrease TER in MDCK C7 cells resulted from its lack of adhesion to other claudins and the consequent formation of breaks in the barrier (Furuse et al., 2001). Although this is a possible mechanism for how induction of claudin-2 might lead to increased pore number, the observed pore size does not change, suggesting that the space created by mismatched claudins is indistinguishable from pores formed in the absence of claudin-2, as seen in the MDCK C7 or Caco-2 cells. Additionally, the increase in pore number was specific for the small pores as we found that overexpression of claudin-2 did not change the flux of mannitol,

and Amasheh and colleagues (Amasheh et al., 2002) found no change in the flux of 4-kDa dextran; both these markers report flux across the size-independent pathway.

In contrast to the effect of expressing claudin-2, the overexpression of claudin-4, -14 and -18 had no effect on pore number or pore size, despite significant effects on TER. This lack of effect could mean that these claudins replace rather than add to existing claudins in the tight junction strands. By substituting for an endogenous claudin that is less ion permeable, expression of these claudins might promote greater electrical tightness, while maintaining the same permeability for nonionic solutes as the endogenous charge-leaky claudin. Similar to the lack of effect of overexpression of claudin-4, knockdown of claudin-2 failed to decrease pore number in MDCK cells. Again, removal of claudin-2 might result in replacement by other claudins that are less cation permeable, resulting in no net change in pore number but resulting in increased TER.

These speculations are not yet supported by experimental evidence as we lack a complete description of claudin expression in MDCK cells and we could observe little compensatory changes in the levels of the other claudins for which we have antibodies. Without an exhaustive comparison of claudin levels, it would be difficult to demonstrate conclusively the difference between substitution and addition, especially as the localization of claudin is not limited to tight junctions, presumably the sites at which they regulate permeability. However, Angelow and colleagues have recently demonstrated that expressed claudin-8 in MDCK II cells replaces endogenous claudin-2 (Angelow et al., 2007), consistent with this possibility.

Some special characteristic of claudin-2 might allow it (and perhaps other as-yet-untested claudins) to be able to add pores. This ability could be related to claudin-2 interactions with cytosolic proteins as preliminary data demonstrate that removal of the C-terminal PDZ-binding motif abrogates the increase in pore number seen with expression of full-length claudin-2 (data not shown). There is also the possibility that expression of claudin-2 acts indirectly to affect pore properties, by affecting a non-claudin pore system or perhaps regulating pore behavior. Several reports have implicated Rho in the regulation of paracellular flux without accompanying changes in TER (Hasegawa et al., 1999), perhaps through the activation of a recently identified tight junction GDP-GTP exchange factor (Benais-Pont et al., 2003). However, a limitation of these studies was their use of markers of higher molecular mass that did not allow measurement of flux through the system of small pores.

In conclusion, PEG profiling reveals several novel insights about the tight junction barrier. A high-capacity pathway for solutes of radius less than 4 Å is responsible for conducting small non-charged solutes and, presumably, small electrolytes. The density of pores along the tight junction varies among cell types and can be increased by expression of claudin-2 but not several other claudins. This, together with their capacity for charge discrimination, implicates claudins in forming the pores but does not rule out a role for other proteins in regulating paracellular flux. It is clear that, although the description of the epithelial barrier properties as 'leaky' or 'tight' is useful, a more accurate characterization of paracellular properties should also take into account the magnitude of both the pore pathway and size-independent pathway and the charge selectivity of the pores. Further studies should be directed at understanding physiologic and pathologic processes that control the characteristics of both pathways.

## Materials and Methods

### Cell culture, immunoblots and immunofluorescence

Caco-2 (BBE cells, kindly provided by M. Mooseker, Yale University, New Haven, CT), T84 (ATCC), LLC-PK<sub>1</sub> cells (kindly provided by J. Mullin, Wistar Institute, Philadelphia, PA) MDCKII (Clontech) and MDCK C7 cells (kindly provided by Hans Oberleithner, Munster, Germany and B. Blazer-Yost, Indiana University Purdue University, Indianapolis, IN) were cultured under standard conditions. Tet-off MDCK II cells expressing human claudin-2 and -4 under a tet-regulated promoter have been described previously (Colegio et al., 2003). MDCK C7 cells expressing claudin-2 (in pcDNA) were generated as described for MDCK II cells; stable cell lines were selected in 1 mg/ml zeocin (InvivoGen, San Diego, CA). Claudin-2-knockdown MDCK II cells were generated using a 19-nucleotide hairpin oligonucleotide claudin-2 sequence described by Hou and colleagues (Hou et al., 2006), cloned into the pTER vector (kindly provided by Marc van der Wetering, Hubrecht Laboratory, Utrecht). Stable cell lines were selected as above in 1 mg/ml zeocin; four independent clones were used for the flux experiments. For flux experiments, cells were plated in parallel at  $1 \times 10^5$  (MDCK and LLC-PK<sub>1</sub>) or  $5 \times 10^5$  (Caco-2 and T84) cells/cm<sup>2</sup> onto removable filters (Snapwell, Corning Life Sciences, Acton, MA) and onto 24 mm, 0.4 µm pore size Transwell filters. MDCK cells were tested 4-8 days after plating; Caco-2 and T84 cells were tested 21 days after plating. Clonal MDCK II cell lines transfected with claudin-2 and -4 were plated in the presence (not induced) or absence (induced) of doxycycline, as described previously (Van Itallie et al., 2003). Determination of TER, mannitol flux, immunoblots and immunofluorescence microscopy of the cultured cells were performed as described previously (Colegio et al., 2002; Van Itallie et al., 2003). All antibodies except the rat monoclonal against ZO-1 (Stevenson et al., 1986) were from Zymed Laboratories (Invitrogen R&D, Carlsbad, CA); Cy-2-, Cy-3- and Cy-5-labeled secondary antibodies for immunofluorescence were from Jackson ImmunoResearch (West Grove, PA) and IR680- and IR800-labeled secondary antibodies for immunoblotting were from Invitrogen and Rockland Immunochemicals (Gilbertsville, PA). The length of the intercellular junction per monolayer area was determined after immunofluorescent labeling of cells with antibodies against ZO-1 (rat monoclonal against ZO-1 for MDCK cells; mouse monoclonal against ZO-1 for human cell lines) in digitally acquired images using Metamorph image analysis software (Meta Imaging Software, Downington, PA).

Porcine ileal mucosa was prepared for barrier function studies as described elsewhere (Gookin et al., 2006); the TER, short circuit current ( $I_{sc}$ ), [<sup>3</sup>H]-mannitol and PEG fluxes were determined. The TER and  $I_{sc}$  were stable throughout two-hour flux studies.

### PEG permeability assay

The polyethylene glycol flux assay was substantially modified from that described by Watson and colleagues (Watson et al., 2001). In place of LC-MS analysis, we adapted a method to modify PEGs fluorescently after the flux protocol with 1-NIC and then resolve the sizes by HPLC and quantify each by fluorescence emission (Rissler et al., 1998). Cell monolayers were rinsed twice at 37°C in Hanks' balanced salt solution (Invitrogen) and preincubated in Hanks' for 30 minutes. The salt solution was removed and replaced with fresh Hanks' or with Hanks' containing a 5 mg/ml mixture of PEG200, PEG400 and PEG900 (Fluka) at a ratio of 2.0:5:1 (by weight). PEGs were added either to the basal or the apical chambers; the level of flux showed no polarity. Samples were removed from the donor and acceptor compartments at 0, 60, 120 and 180 minutes and an internal standard (20 µg purified PEG28, Polypure AS, Oslo, Norway) was added to all samples. After storage at -20°C, samples were thawed and dried at 55°C in a water bath under a stream of N<sub>2</sub>. PEGs were derivatized by addition of 10 µl 1-NIC (Acros Organics) in 100 µl of acetone. Samples were vortexed for 4 hours at room temperature; then 50 µl of methanol and 500 µl H<sub>2</sub>O were added to quench excess reagent and samples were vortexed vigorously. Following two extractions with diethylether, 100 µl of the aqueous phase was analyzed on a bare silica column (Waters Spherisorb 5.0 µm Silica column, 4.6×150 mm, Waters Corporation, Milford, MA) by HPLC (Agilent Technologies) and peaks quantified by fluorescence emission (Agilent HPCHEM station, excitation=232 nm, emission=358 nm).  $P_{app}$  was determined as  $(dQ/dt)/A \times C_0$  where A=filter area and C<sub>0</sub> is the initial concentration in the donor compartment. C<sub>0</sub> did not change significantly over the 120 minute flux study.

To correct the  $P_{app}$  of the size-dependent first phase, the second phase is extended after linear regression and subtracted from the first phase. The aqueous pore radius was calculated from the ratio of the corrected paracellular permeabilities of pairs of two small PEG species (2.8, 3.2, 3.5 or 3.7), applying a sieving function as described in equations 7 (see Renken, 1954) and 8 (see Knipp et al., 1997). Corrected values for the 3.2 or 3.5 Å species were used to compare flux in Figs 3 and 5 and represent the permeability for a size that freely permeates the pore.

We thank Alan Fanning for helpful discussions and Erika Wittchen and Keith Burridge for HUVECs. This work was supported by NIH grants DK45134 (to J.M.A.) and P30 DK 034987 and DK070883 (to J.G.).

## References

- Alexandre, M. D., Jeansonne, B. G., Renegar, R. H., Tatum, R. and Chen, Y. H. (2007). The first extracellular domain of claudin-7 affects paracellular Cl<sup>-</sup> permeability. *Biochem. Biophys. Res. Commun.* **357**, 87-91.
- Amasheh, S., Meiri, N., Gitter, A. H., Schoneberg, T., Mankertz, J., Schulzke, J. D. and Fromm, M. (2002). Claudin-2 expression induces cation-selective channels in tight junctions of epithelial cells. *J. Cell Sci.* **115**, 4969-4976.
- Angelow, S., Schneeberger, E. E. and Yu, A. S. (2007). Claudin-8 expression in renal epithelial cells augments the paracellular barrier by replacing endogenous claudin-2. *J. Membr. Biol.* **215**, 147-159.
- Artursson, P., Ungell, A. L. and Lofroth, J. E. (1993). Selective paracellular permeability in two models of intestinal absorption: cultured monolayers of human intestinal epithelial cells and rat intestinal segments. *Pharm. Res.* **10**, 1123-1129.
- Balda, M. S., Whitney, J. A., Flores, C., Gonzalez, S., Cerejido, M. and Matter, K. (1996). Functional dissociation of paracellular permeability and transepithelial electrical resistance and disruption of the apical-basolateral intramembrane diffusion barrier by expression of a mutant tight junction membrane protein. *J. Cell Biol.* **134**, 1031-1049.
- Ben Yosef, T., Belyantseva, I. A., Saunders, T. L., Hughes, E. D., Kawamoto, K., Van Itallie, C. M., Beyer, L. A., Halsey, K., Gardner, D. J., Wilcox, E. R. et al. (2003). Claudin 14 knockout mice, a model for autosomal recessive deafness DFNB29, are deaf due to cochlear hair cell degeneration. *Hum. Mol. Genet.* **12**, 2049-2061.
- Benais-Pont, G., Punna, A., Flores-Maldonado, C., Eckert, J., Raposo, G., Fleming, T. P., Cerejido, M., Balda, M. S. and Matter, K. (2003). Identification of a tight junction-associated guanine nucleotide exchange factor that activates Rho and regulates paracellular permeability. *J. Cell Biol.* **160**, 729-740.
- Claude, P. (1978). Morphological factors influencing transepithelial permeability: a model for the resistance of the zonula occludens. *J. Membr. Biol.* **39**, 219-232.
- Colegio, O. R., Van Itallie, C. M., McCrea, H. J., Rahner, C. and Anderson, J. M. (2002). Claudins create charge-selective channels in the paracellular pathway between epithelial cells. *Am. J. Physiol. Cell Physiol.* **283**, C142-C147.
- Colegio, O. R., Van Itallie, C., Rahner, C. and Anderson, J. M. (2003). Claudin extracellular domains determine paracellular charge selectivity and resistance but not tight junction fibril architecture. *Am. J. Physiol. Cell Physiol.* **284**, C1346-C1354.
- Fihn, B. M., Sjoqvist, A. and Jodal, M. (2000). Permeability of the rat small intestinal epithelium along the villus-crypt axis: effects of glucose transport. *Gastroenterology* **119**, 1029-1036.
- Furuse, M., Hirase, T., Itoh, M., Nagafuchi, A., Yonemura, S., Tsukita, S. and Tsukita, S. (1993). Occludin: a novel integral membrane protein localizing at tight junctions. *J. Cell Biol.* **123**, 1777-1788.
- Furuse, M., Sasaki, H., Fujimoto, K. and Tsukita, S. (1998). A single gene product, claudin-1 or -2, reconstitutes tight junction strands and recruits occludin in fibroblasts. *J. Cell Biol.* **143**, 391-401.
- Furuse, M., Furuse, K., Sasaki, H. and Tsukita, S. (2001). Conversion of zonulae occludentes from tight to leaky strand type by introducing claudin-2 into Madin-Darby canine kidney I cells. *J. Cell Biol.* **153**, 263-272.
- Gekle, M., Wunsch, S., Oberleithner, H. and Silbernagl, S. (1994). Characterization of two MDCK-cell subtypes as a model system to study principal cell and intercalated cell properties. *Pflügers Arch.* **428**, 157-162.
- Ghandehari, H., Smith, P. L., Ellens, H., Yeh, P. Y. and Kopecek, J. (1997). Size-dependent permeability of hydrophilic probes across rabbit colonic epithelium. *J. Pharmacol. Exp. Ther.* **280**, 747-753.
- Gonzalez-Mariscal, L., Betanzos, A., Nava, P. and Jaramillo, B. E. (2003). Tight junction proteins. *Prog. Biophys. Mol. Biol.* **81**, 1-44.
- Gookin, J. L., Chiang, S., Allen, J., Armstrong, M. U., Stauffer, S. H., Finnegan, C. and Murtaugh, M. P. (2006). NF-kappaB-mediated expression of iNOS promotes epithelial defense against infection by *Cryptosporidium parvum* in neonatal piglets. *Am. J. Physiol. Gastrointest. Liver Physiol.* **290**, G164-G174.
- Hasegawa, H., Fujita, H., Katoh, H., Aoki, J., Nakamura, K., Ichikawa, A. and Negishi, M. (1999). Opposite regulation of transepithelial electrical resistance and paracellular permeability by Rho in Madin-Darby canine kidney cells. *J. Biol. Chem.* **274**, 20982-20988.
- He, Y. L., Murby, S., Warhurst, G., Gifford, L., Walker, D., Ayrton, J., Eastmond, R. and Rowland, M. (1998). Species differences in size discrimination in the paracellular pathway reflected by oral bioavailability of poly(ethylene glycol) and D-peptides. *J. Pharm. Sci.* **87**, 626-633.
- Hille, B. (2001). *Ion Channels of Excitable Membranes*. Sunderland, MA: Sinauer Associates.
- Holmes, J. L., Van Itallie, C. M., Rasmussen, J. E. and Anderson, J. M. (2006). Claudin profiling in the mouse during postnatal intestinal development and along the gastrointestinal tract reveals complex expression patterns. *Gene Expr. Patterns* **6**, 581-588.
- Hou, J., Paul, D. L. and Goodenough, D. A. (2005). Paracellin-1 and the modulation of ion selectivity of tight junctions. *J. Cell Sci.* **118**, 5109-5118.
- Hou, J., Gomes, A. S., Paul, D. L. and Goodenough, D. A. (2006). Study of claudin function by RNA interference. *J. Biol. Chem.* **281**, 36117-36123.
- Itoh, M., Sasaki, H., Furuse, M., Ozaki, H., Kita, T. and Tsukita, S. (2001). Junctional adhesion molecule (JAM) binds to PAR-3: a possible mechanism for the recruitment of PAR-3 to tight junctions. *J. Cell Biol.* **154**, 491-497.
- Knipp, G. T., Ho, N. F., Barsuhn, C. L. and Borchardt, R. T. (1997). Paracellular diffusion in Caco-2 cell monolayers: effect of perturbation on the transport of hydrophilic compounds that vary in charge and size. *J. Pharm. Sci.* **86**, 1105-1110.
- Mandell, K. J. and Parkos, C. A. (2005). The JAM family of proteins. *Adv. Drug Deliv. Rev.* **57**, 857-867.

- Marcial, M. A., Carlson, S. L. and Madara, J. L.** (1984). Partitioning of paracellular conductance along the ileal crypt-villus axis: a hypothesis based on structural analysis with detailed consideration of tight junction structure-function relationships. *J. Membr. Biol.* **80**, 59-70.
- Notterpek, L., Roux, K. J., Amici, S. A., Yazdanpour, A., Rahner, C. and Fletcher, B. S.** (2001). Peripheral myelin protein 22 is a constituent of intercellular junctions in epithelia. *Proc. Natl. Acad. Sci. USA* **98**, 14404-14409.
- Powell, D. W.** (1981). Barrier function of epithelia. *Am. J. Physiol.* **241**, G275-G288.
- Renken, E.** (1954). Filtration, diffusion, and molecular sieving through porous cellulose membranes. *J. Gen. Physiol.* **20**, 225-243.
- Rissler, K., Wyttenbach, N. and Börnsen, K.** (1998). High-performance liquid chromatography of polyethylene glycols as their 1-naphthylurethane derivatives and signal monitoring by fluorescence detection. *J. Chromatogr. A* **822**, 189-206.
- Ruddy, S. B. and Hadzija, B. W.** (1992). Ionophoretic permeability of polyethylene glycols through hairless rat skin: application of hydrodynamic theory for hindered transport through liquid-filled pores. *Drug Des. Discov.* **8**, 207-224.
- Saitou, M., Fujimoto, K., Doi, Y., Itoh, M., Fujimoto, T., Furuse, M., Takano, H., Noda, T. and Tsukita, S.** (1998). Occludin-deficient embryonic stem cells can differentiate into polarized epithelial cells bearing tight junctions. *J. Cell Biol.* **141**, 397-408.
- Sanders, S. E., Madara, J. L., McGuirk, D. K., Gelman, D. S. and Colgan, S. P.** (1995). Assessment of inflammatory events in epithelial permeability: a rapid screening method using fluorescein dextrans. *Epithelial Cell Biol.* **4**, 25-34.
- Schneeberger, E. E. and Lynch, R. D.** (2004). The tight junction: a multifunctional complex. *Am. J. Physiol. Cell Physiol.* **286**, C1213-C1228.
- Stevenson, B. R., Siliciano, J. D., Mooseker, M. S. and Goodenough, D. A.** (1986). Identification of ZO-1: a high molecular weight polypeptide associated with the tight junction (zonula occludens) in a variety of epithelia. *J. Cell Biol.* **103**, 755-766.
- Stevenson, B. R., Anderson, J. M., Goodenough, D. A. and Mooseker, M. S.** (1988). Tight junction structure and ZO-1 content are identical in two strains of Madin-Darby canine kidney cells which differ in transepithelial resistance. *J. Cell Biol.* **107**, 2401-2408.
- Tavelin, S., Taipalensuu, J., Soderberg, L., Morrison, R., Chong, S. and Artursson, P.** (2003). Prediction of the oral absorption of low-permeability drugs using small intestine-like 2/4/A1 cell monolayers. *Pharm. Res.* **20**, 397-405.
- Van Itallie, C., Rahner, C. and Anderson, J. M.** (2001). Regulated expression of claudin-4 decreases paracellular conductance through a selective decrease in sodium permeability. *J. Clin. Invest.* **107**, 1319-1327.
- Van Itallie, C. M., Fanning, A. S. and Anderson, J. M.** (2003). Reversal of charge selectivity in cation or anion-selective epithelial lines by expression of different claudins. *Am. J. Physiol. Renal Physiol.* **285**, F1078-F1084.
- Watson, C. J., Rowland, M. and Warhurst, G.** (2001). Functional modeling of tight junctions in intestinal cell monolayers using polyethylene glycol oligomers. *Am. J. Physiol. Cell Physiol.* **281**, C388-C397.
- Watson, C. J., Hoare, C. J., Garrod, D. R., Carlson, G. L. and Warhurst, G.** (2005). Interferon-gamma selectively increases epithelial permeability to large molecules by activating different populations of paracellular pores. *J. Cell Sci.* **118**, 5221-5230.
- Wunsch, S., Gekle, M., Kersting, U., Schuricht, B. and Oberleithner, H.** (1995). Phenotypically and karyotypically distinct Madin-Darby canine kidney cell clones respond differently to alkaline stress. *J. Cell. Physiol.* **164**, 164-171.
- Yu, A. S., Enck, A. H., Lencer, W. I. and Schneeberger, E. E.** (2003). Claudin-8 expression in Madin-Darby canine kidney cells augments the paracellular barrier to cation permeation. *J. Biol. Chem.* **278**, 17350-17359.
- Yu, A. S., McCarthy, K. M., Francis, S. A., McCormack, J. M., Lai, J., Rogers, R. A., Lynch, R. D. and Schneeberger, E. E.** (2005). Knockdown of occludin expression leads to diverse phenotypic alterations in epithelial cells. *Am. J. Physiol. Cell Physiol.* **288**, C1231-C1241.